Geophysical Journal International

Geophys. J. Int. (2012) **188,** 631–644 doi: 10.1111/j.1365-246X.2011.05286.x

A time-domain recursive method to analyse transient wave propagation across rock joints

J. C. Li,[1] H.B. Li,[1] G. W. Ma[2] and J. Zhao[3]

[1] *State Key Laboratory of Geomechanics and Geotechnical Engineering, Institute of Rock and Soil Mechanics, Chinese Academy of Sciences, Wuhan* 430071, *China. E-mail: jcli@whrsm.ac.cn*
[2] *School of Civil and Resource Engineering, University of Western Australia,* 35 *Stirling Highway, Crawley* WA6009, *Australia*
[3] *Ecole Polytechnique Fédérale de Lausanne (EPFL), Laboratory for Rock Mechanics (LMR),* CH-1015 *Lausanne, Switzerland*

Accepted 2011 October 30. Received 2011 October 30; in original form 2011 August 25

SUMMARY

The present investigation is concerned with transient wave propagation in a rock mass with a set of parallel joints by using a recursive method. According to the displacement field of a rock mass with a set of parallel joints, the interaction between four plane waves (two longitudinal-waves and two transverse-waves) and a joint is analysed first. With the displacement discontinuity model and the time shifting function, the wave propagation equation based on the recursive method in time domain for obliquely longitudinal-(P) or transverse-(S) waves across a set of parallel joints is established. The joints are assumed linearly elastic. The analytical solution obtained by the proposed method is compared with the existing results for some special cases, including oblique incidence across a single joint and normal incidence across a set of parallel joints. By verification, it is found that the solutions by the proposed method match very well with the existing methods. The applicability and limitations of the new method are then discussed for incident waves with different properties.

Key words: Time-series analysis; Body waves; Seismic attenuation; Wave propagation; Fractures and faults.

1 INTRODUCTION

Studying transient wave propagation across rock masses is an important topic, which has received considerable attention in geophysics, mining and underground constructions. A rock mass usually consists of multiple, parallel planar joints, known as joint sets, which not only govern the mechanical behaviour of the rock mass but also affect the wave propagation in the rock mass. Because of the discontinuity in nature, the wave propagation across rock joints becomes a complicated process. Therefore, it is of significance to develop an efficient and explicit method to analyse this process.

Generally, three methods are available for studies on wave propagation across a jointed rock mass. One is the numerical modelling, which provides a convenient and economical approach, especially for complicated geological cases. However, representation of the joints in the numerical models presents a great challenge. The experimental study is the second method, which is sometimes limited by the existing test techniques. The third is the theoretical study from which the mechanism and the process of wave propagation across a jointed rock mass can be revealed for some special geological cases. Meanwhile, the analytical study can provide an estimate and reference for the lab and/or the field tests to some extent.

Analytical studies for an incident P- or S-wave propagation across a discontinuous interface have been extensively conducted by many researchers. Kolsky (1953) derived the relation between the wave propagation speeds and the emergence angles of the reflected and refracted waves for a discontinuous interface between two media, which is also termed as the Snell's law. On the basis of the displacement discontinuity model and the Snell's law, propagation of oblique wave incidence across a planar linear slip interface was investigated by Schoenberg (1980). Later, the close-form solutions for a harmonic incidence across a rock joint were obtained and expressed in a matrix form subsequently derived by Pyrak-Nolte *et al*. (1990a,b), Gu *et al.* (1996) and Zhu *et al.* (2011). The above methods were based on the fundamental solutions of the equation of motion. Based on the characteristic line theory (Ewing *et al.* 1957; Bedford & Drumheller 1994) and the displacement discontinuity model (Miller 1977; Schoenberg 1980), Zhao and Cai (2001) calculated the transmission coefficient of incident P waves across a single rock joint. Considering the balance of momentum at the wave front and the displacement discontinuity model, Li and Ma (2010) analysed the interaction between a blast-induced wave and a rock joint with arbitrary impinging angle.

Normally incident waves across a set of joints have also been investigated by a number of researchers. For example, Zhao *et al.* (2006a,b) adopted the characteristic line theory to derive a wave propagation equation in time domain, which can be applied for analysing normally incident *P* and *S* waves with an arbitrary waveform. With a transmission line formula, the scattering matrix method (SMM; Aki & Richards 2002; Perino *et al.* 2010) was used to study harmonic wave propagation across a set of parallel joints. By considering the rock mass as an equivalent viscoelastic medium, Li *et al.* (2010) analysed the normally incident *P*-wave propagation across a set of rock joints.

Compared to the normal case and the case of an oblique incidence across a single joint, the analysis for an incident wave across a number of rock joints is much more complicated, due to the new kinds of wave produced from the joint interface and multiple wave reflections among the joints. The multiple reflections have been recognized to have significant effects on the reflected and transmitted waves in jointed rock masses (Pyrak-Nolte *et al.* 1990b). A reflection method (Fuchs & Müller 1971) and a propagator method (Kennett & Kerry 1979; Luco & Apsel 1983) were presented to study an incidence travelling obliquely in a periodical layered medium. These two methods can establish the relation among different layers with respect to the reflection and transmission amplitudes and the corresponding phase shift, which were expressed in frequency domain. For an incident wave with arbitrary waveform, it is necessary to use the Fourier synthesis over frequency in the two methods.

This study is motivated by the need to better understand the role of a set of parallel joints on the transient wave propagation and how relevant parameters play their roles on the transmission and reflection. The transient waves are longitudinal-(*P*) or transverse-(*S*) waves, and their interaction with a linearly elastic rock joint is first analysed. According to the time-shifting function of the *P* and *S* waves between two adjacent joints and a recursive method in time domain, the wave propagation equation across rock joints is established for arbitrary impinging angle. The special cases, such as the normal incidence across joints and the oblique incidence across a single joint are also investigated. The calculations for some special cases are compared with the existing results. Finally, the applicability and limitations of the proposed method are discussed.

2 TIME-DOMAIN RECURSIVE METHOD

2.1 Problem description

We consider a homogeneous, isotropic and linearly elastic rock which contains a set of parallel joints, as shown in Fig. 1, where N denotes the joint number. Each joint is considered as a non-welded contact interface, which is planar, large in extent and small in thickness compared to the wavelength. The joints are linearly elastic, lying in the x–z plane and extend to infinity in the x–y plane. The joints behave linearly with normal stiffness k_n and shear stiffness k_s, and the spacing between two adjacent joints is S. For the intact rock, μ and ν denote the shear modulus and the Poisson's ratio, ρ is the density, and c_p and c_s are the velocities of *P* and *S* waves, respectively.

In an ideally elastic rock, the displacement field for a 2-D problem is expressed in terms of a scalar potential φ and a vector potential ψ (Achenbach 1973), which correspond to uncoupled longitudinal-(*P*-) and shear-(*S*-)waves propagation, respectively. An incident plane wave of either *P*- or *S*-wave travels in the x–z plane. When an incident wave impinges on the interface of a discontinuity, both reflection and transmission take place (Kolsky 1953). Define α and β as the emergence angles of the incident *P* and *S* waves, respectively, and α_c and β_c as the critical angles of the incident *P* and *S* waves, respectively. Then, $0 \leq \alpha < \alpha_c$ and $0 \leq \beta < \beta_c$, where $\alpha_c = 90^\circ$ and $\beta_c = \sin^{-1}(c_s/c_p)$ from the Snell's law.

For the rock mass with a set of parallel joints, the rock materials between joints are identical. According to the Snell's law, the emergence angles of the reflected and transmitted waves are equal to the incident angles. In another word, if the emergence angle of the incident *P* wave is α, the angles of the reflected and transmitted *P* waves are also equal to α, so are the emergence angles of the incident, reflected and transmitted *S* waves. For the present problem, when the incident wave propagates in a rock mass and is reflected multiple times among the joints, there exist four waves propagating in four directions in the rock mass, that is, the right-running *P* and *S* waves and left-running *P* and *S* waves, which are shown in Fig. 2. The four waves along four directions across multiple parallel joints were also illustrated in the researches

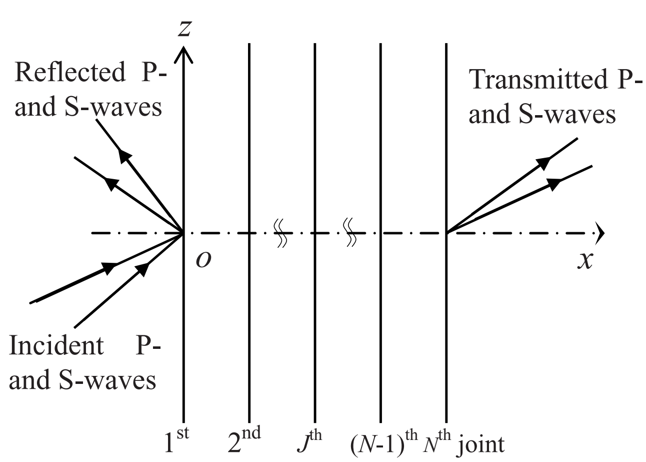

Figure 1. Incident *P* wave upon a rock mass with a set of parallel joints.

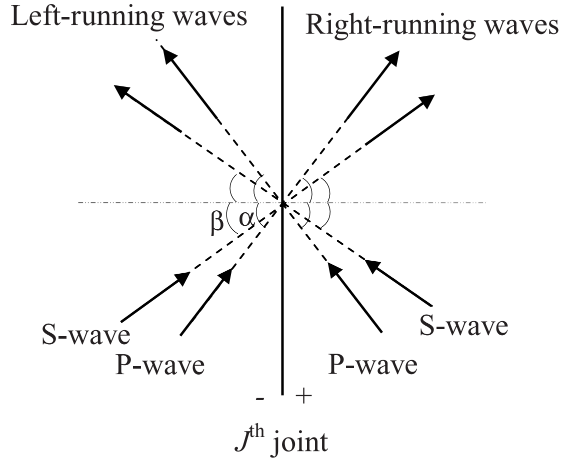

Figure 2. Schematic view of left- and right-running *P* and *S* waves in a rock mass.

by Pyrak-Nolte *et al.* (1990a,b) and Gu *et al.* (1996). For a joint, such as the *J*th joint in the rock mass, the right- and left-running *P* waves are symmetric with respect to the joint, so are the right- and left-running *S* waves.

2.2 Interaction between stress waves and rock joint

As illustrated in Fig. 3(a), when a beam of right-running *P*-wave impinges the left-hand side of the *J*th joint, there is a tiny element *ABC* delimited by the left-hand side of the joint, the wave front and the side of the wave beam. Similarly, the other left- and right-running *P* and *S* waves also give rise to the other tiny elements, as shown in Figs 3(b)–(h), when the waves arrive at two sides of the joint. In Fig. 3, σ_{rp}^m and σ_{lp}^m denote the normal stresses of the right- and left-running *P* waves on their wave fronts, τ_{rp}^m and τ_{lp}^m denote the shear stresses of the right-

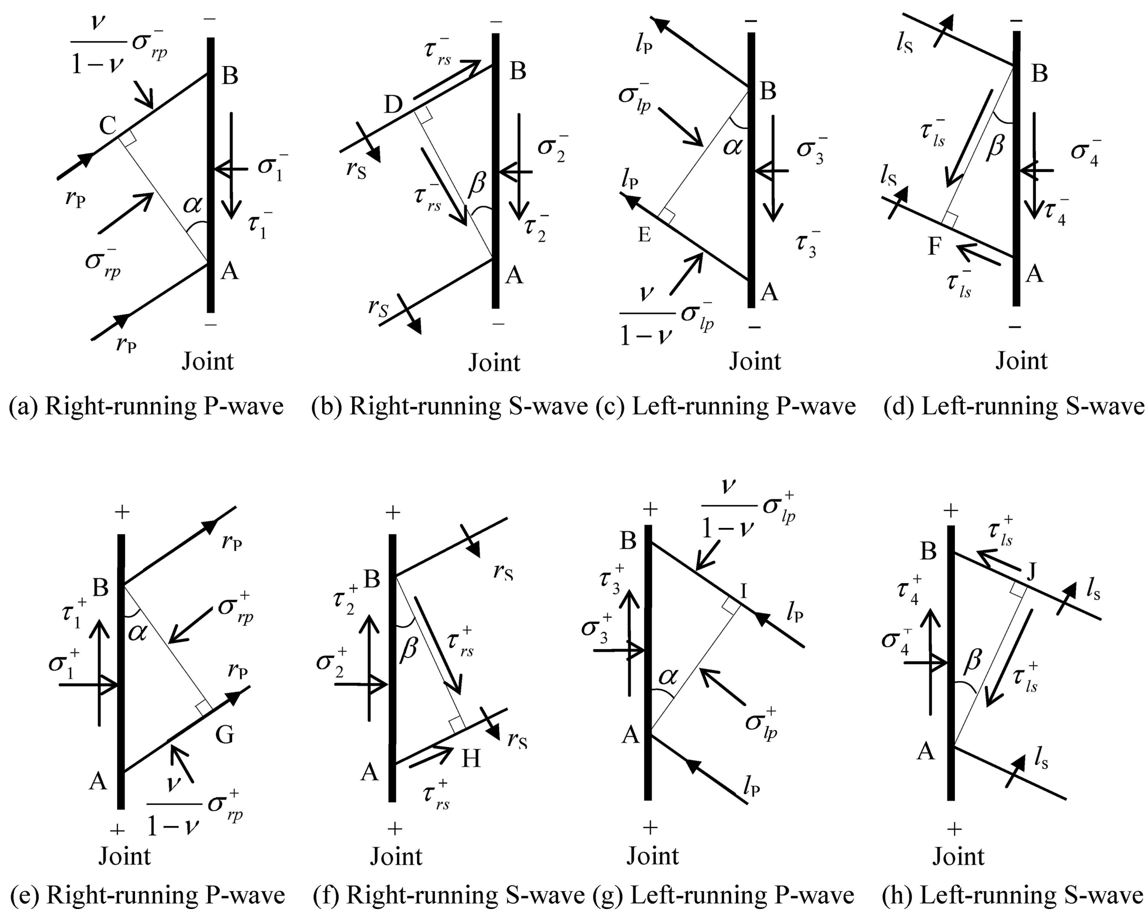

Figure 3. Stresses and right- and left-running waves on the two sides of a joint.

and left-running S waves on their wave fronts, where m represents the symbols '–' and '+' which indicate the left- and right-hand sides of the Jth joint, respectively. Since the present problem is a plane strain problem, the stresses on the beam sides of the right- and left-running P waves are $\frac{v}{1-v}\sigma_{rp}^m$ and $\frac{v}{1-v}\sigma_{lp}^m$, respectively. If the body force is not considered, the normal and tangential components of stresses, that is, σ_q^m and τ_q^m ($q = 1{\sim}4$, $m = -, +$) on the left- and right-hand sides of the Jth joint can be derived according to Li & Ma (2010), that is,

$$\sigma_1^m = \sigma_{rp}^m \cos 2\beta, \quad \tau_1^m = \sigma_{rp}^m \sin 2\beta \tan 2\beta / \tan\alpha \tag{1}$$

$$\sigma_2^m = \tau_{rs}^m \sin 2\beta, \quad \tau_2^m = -\tau_{rs}^m \cos 2\beta \tag{2}$$

$$\sigma_3^m = \sigma_{lp}^m \cos 2\beta, \quad \tau_3^m = -\sigma_{lp}^m \sin 2\beta \tan\beta / \tan\alpha \tag{3}$$

$$\sigma_4^m = -\tau_{ls}^m \sin 2\beta, \quad \tau_4^m = -\tau_{ls}^m \cos 2\beta. \tag{4}$$

The normal and tangential stresses, σ^- and τ^-, on the left-hand side of the Jth joint can be obtained from the superposition of σ_q^- and τ_q^- ($q = 1{\sim}4$), respectively, or $\sigma^- = \sum_{q=1}^4 \sigma_q^-$ and $\tau^- = \sum_{q=1}^4 \tau_q^-$. The normal and tangential stresses, σ^+ and τ^+, on the right-hand side of the Jth joint can also be obtained from eqs (1) to (4). v_p and v_s are defined as the particle velocities of P and S waves, respectively, and z_p and z_s as ρc_p and ρc_s, respectively. According to the balance of momentum on the wave fronts, the stresses on the wave fronts of P and S waves can be written as

$$\sigma_p = z_p v_p \quad \text{and} \quad \tau_s = z_s v_s. \tag{5}$$

When eq. (5) is substituted into eqs (1)–(4), σ^m and τ^m ($m = -, +$) on the two sides of the Jth joint can be rewritten as

$$\sigma^- = (z_p \cos 2\beta)v_{rp}^- + (z_s \sin 2\beta)v_{rs}^- + (z_p \cos 2\beta)v_{lp}^- + (-z_s \sin 2\beta)v_{ls}^- \tag{6}$$

$$\tau^- = (z_p \sin 2\beta \tan\beta/\tan\alpha)v_{rp}^- + (-z_s \cos 2\beta)v_{rs}^- + (-z_p \sin 2\beta \tan\beta/\tan\alpha)v_{lp}^- + (-z_s \cos 2\beta)v_{ls}^- \tag{7}$$

$$\sigma^+ = (z_p \cos 2\beta)v_{rp}^+ + (z_s \sin 2\beta)v_{rs}^+ + (z_p \cos 2\beta)v_{lp}^+ + (-z_s \sin 2\beta)v_{ls}^+ \tag{8}$$

$$\tau^+ = (z_p \sin 2\beta \tan\beta/\tan\alpha)v_{rp}^+ + (-z_s \cos 2\beta)v_{rs}^+ + (-z_p \sin 2\beta \tan\beta/\tan\alpha)v_{lp}^+ + (-z_s \cos 2\beta)v_{ls}^+, \tag{9}$$

where v_{rp}^m and v_{lp}^m ($m = -, +$) are the particle velocities of right- and left-running P waves on the two sides of the joint, respectively; and v_{rs}^m and v_{rs}^m ($m = -, +$) are the particle velocities of right- and left-running S waves on the two sides of the joint, respectively.

It is noted from Fig. 3 that the normal and tangential components of the velocity before the left-hand side of the Jth joint are

$$v_n^- = \cos\alpha\, v_{rp}^- + \sin\beta\, v_{rs}^- - \cos\alpha\, v_{lp}^- + \sin\beta\, v_{ls}^- \tag{10}$$

$$v_\tau^- = \sin\alpha\, v_{rp}^- - \cos\beta\, v_{rs}^- + \sin\alpha\, v_{lp}^- + \cos\beta\, v_{ls}^- \tag{11}$$

and the normal and tangential components of the velocity after the right-hand side of the Jth joint are

$$v_n^+ = \cos\alpha\, v_{rp}^+ + \sin\beta\, v_{rs}^+ - \cos\alpha\, v_{lp}^+ + \sin\beta\, v_{ls}^+ \tag{12}$$

$$v_\tau^+ = \sin\alpha\, v_{rp}^+ - \cos\beta\, v_{rs}^+ + \sin\alpha\, v_{lp}^+ + \cos\beta\, v_{ls}^+ \tag{13}$$

2.3 Wave propagation equation

For the Jth joint, the stresses and the displacements before and after the two sides of the joint should satisfy the displacement discontinuous boundary condition (Miller 1977; Schoenberg 1980), that is,

$$\sigma^- = \sigma^+ = \sigma, \quad \tau^- = \tau^+ = \tau, \tag{14}$$

$$u_n^- - u_n^+ = \frac{\sigma}{k_n}, \quad u_\tau^- - u_\tau^+ = \frac{\tau}{k_s}, \tag{15}$$

where k_n and k_s are the normal and tangential stiffness of the joint; u_n^- and u_n^+ are the normal displacement before and after the two sides of the joint, respectively; u_τ^- and u_τ^+ are the shear displacement before and after the two sides of the joint, respectively. When eq. (15) is differential with respect to time t, there is

$$v_{n(i)}^- - v_{n(i)}^+ = \frac{1}{k_n}\frac{\partial\sigma}{\partial t} = \frac{1}{k_n}\frac{\sigma_{(i+1)} - \sigma_{(i)}}{\Delta t}, \quad v_{\tau(i)}^- - v_{\tau(i)}^+ = \frac{1}{k_s}\frac{\partial\tau}{\partial t} = \frac{1}{k_s}\frac{\tau_{(i+1)} - \tau_{(i)}}{\Delta t}, \tag{16}$$

where Δt is a small time interval. The relations for the P and S waves between two adjacent joints must satisfy the time-shifting function, or

$$v_{rp,J}^-(t) = v_{rp,J-1}^+\left(t - \frac{S}{\cos\alpha \cdot c_p}\right), \quad v_{rs,J}^-(t) = v_{rs,J-1}^+\left(t - \frac{S}{\cos\beta \cdot c_s}\right) \tag{17}$$

$$v_{lp,J}^+(t) = v_{lp,J+1}^-\left(t - \frac{S}{\cos\alpha \cdot c_p}\right), \quad v_{ls,J}^+(t) = v_{ls,J+1}^-\left(t - \frac{S}{\cos\beta \cdot c_s}\right), \tag{18}$$

where 'J–1' and 'J+1' denote the (J–1)th and (J+1)th joints in the rock mass, respectively. Eq. (17) for the P and S waves between two adjacent joints implies that the right-running P or S wave, v_{rp}^- or v_{rs}^-, on the left-hand side of the Jth joint keeps zero before v_{rp}^+ or v_{rs}^+ emitted from the right-hand side of the (J–1)th joint arrives at the Jth joint. Similarly, eq. (18) shows that the left-running P or S wave, v_{lp}^+ or v_{ls}^+, on the right-hand side of the Jth joint is zero until the arrival of v_{rp}^- or v_{rs}^- caused from the left-hand side of the (J+1)th joint. In the following analysis, the shifting times for the P and S waves between two adjacent joints are scattered as n_p and n_s, respectively, which are the integers of $S/(\cos\alpha \cdot c_p \cdot \Delta t)$ and $S/(\cos\beta \cdot c_s \cdot \Delta t)$, or $n_p = \mathrm{int}[S/(\cos\alpha \cdot c_p \cdot \Delta t)]$ and $n_s = \mathrm{int}[S/(\cos\beta \cdot c_s \cdot \Delta t)]$.

When eqs (6)–(13) are combined with eqs (14) and (16), the wave propagation equation across the Jth joint can be derived and expressed as a matrix form

$$\begin{bmatrix} v_{lp}^- \\ v_{ls}^- \end{bmatrix}_{i,J} = -B^{-1}A \begin{bmatrix} v_{rp}^- \\ v_{rs}^- \end{bmatrix}_{i,J} + B^{-1}A \begin{bmatrix} v_{rp}^+ \\ v_{rs}^+ \end{bmatrix}_{i,J} + \begin{bmatrix} v_{lp}^+ \\ v_{ls}^+ \end{bmatrix}_{i,J} \tag{19}$$

$$\begin{bmatrix} v_{rp}^+ \\ v_{rs}^+ \end{bmatrix}_{i+1,J} = -A^{-1}B \begin{bmatrix} v_{lp}^+ \\ v_{ls}^+ \end{bmatrix}_{i+1,J} + A^{-1}C \begin{bmatrix} v_{rp}^+ \\ v_{rs}^+ \end{bmatrix}_{i,J} + A^{-1}D \begin{bmatrix} v_{lp}^+ \\ v_{ls}^+ \end{bmatrix}_{i,J} + A^{-1}E \begin{bmatrix} v_{rp}^- \\ v_{rs}^- \end{bmatrix}_{i,J} + A^{-1}F \begin{bmatrix} v_{lp}^- \\ v_{ls}^- \end{bmatrix}_{i,J} . \tag{20}$$

Considering the time-shifting functions (17) and (18), the waves between two adjacent joints are written as

$$\begin{bmatrix} v_{rp}^- \\ v_{rs}^- \end{bmatrix}_{i,J} = \begin{bmatrix} v_{rp}^+ \\ v_{rs}^+ \end{bmatrix}_{i-n_p,J-1} , \quad \begin{bmatrix} v_{lp}^+ \\ v_{ls}^+ \end{bmatrix}_{i,J} = \begin{bmatrix} v_{lp}^- \\ v_{ls}^- \end{bmatrix}_{i-n_p,J+1} , \tag{21}$$

where A to F are the matrix parameters shown as

$$A = \begin{bmatrix} z_p \cos 2\beta & z_s \sin 2\beta \\ z_p \sin 2\beta \tan\beta / \tan\alpha & -z_s \cos 2\beta \end{bmatrix} \tag{22}$$

$$B = \begin{bmatrix} z_p \cos 2\beta & -z_s \sin 2\beta \\ -z_p \sin 2\beta \tan\beta / \tan\alpha & -z_s \cos 2\beta \end{bmatrix} \tag{23}$$

$$C = \begin{bmatrix} z_p \cos 2\beta - k_n \Delta t \cos\alpha & z_s \sin 2\beta - k_n \Delta t \sin\beta \\ z_p \sin 2\beta \tan\beta / \tan\alpha - k_s \Delta t \sin\alpha & -z_s \cos 2\beta + k_s \Delta t \cos\beta \end{bmatrix} \tag{24}$$

$$D = \begin{bmatrix} z_p \cos 2\beta + k_n \Delta t \cos\alpha & -z_s \sin 2\beta - k_n \Delta t \sin\beta \\ -z_p \sin 2\beta \tan\beta / \tan\alpha - k_s \Delta t \sin\alpha & -z_s \cos 2\beta - k_s \Delta t \cos\beta \end{bmatrix} \tag{25}$$

$$E = \begin{bmatrix} k_n \Delta t \cos\alpha & k_n \Delta t \sin\beta \\ k_s \Delta t \sin\alpha & -k_s \Delta t \cos\beta \end{bmatrix} \tag{26}$$

$$F = \begin{bmatrix} -k_n \Delta t \cos\alpha & k_n \Delta t \sin\beta \\ k_s \Delta t \sin\alpha & k_s \Delta t \cos\beta \end{bmatrix} . \tag{27}$$

Eqs (19)–(21) are the recursive equations for an incident P- or S-wave propagation across a set of parallel rock joints. The wave propagation eqs (19)–(21) include two portions: one is eqs (19) and (20) for wave propagation across a joint and another is the time-shifting function (21) for wave propagation between two adjacent joints.

2.4 Calculating steps

If the incident P or S wave in Fig. 1 is $I_p(t)$ or $I_s(t)$, there is $[\, v_{rp}^- \; v_{rs}^- \,]_{i,1}^T = [\, I_p \; 0 \,]_{i,1}^T$ or $[\, v_{rp}^- \; v_{rs}^- \,]_{i,1}^T = [\, 0 \; I_s \,]_{i,1}^T$ in eqs (19) and (20) for the first joint or $J = 1$, where the symbol 'T' denotes the matrix transpose. The initial condition is that the left- and right-running P and S wave are zero except $[\, v_{rp}^- \; v_{rs}^- \,]_{i,1}^T$ equal to the incident wave.

First, at time i, the left-running P and S waves, v_{lp}^+ and v_{ls}^+, on the right-hand side of the first joint can be obtained from the left-running P and S waves, v_{lp}^- and v_{ls}^-, on the left-hand side of the second joint, that is, $[\, v_{lp}^+ \; v_{ls}^+ \,]_{i,1}^T = [\, v_{lp}^- \; v_{ls}^- \,]_{i-n_p,2}^T$ from Eq. (21). Similarly, $[\, v_{lp}^+ \; v_{ls}^+ \,]_{i+1,1}^T$ for time $i+1$ can also be obtained. According to the initial condition and the incidence, the right-running P and S waves $[\, v_{rp}^+ \; v_{rs}^+ \,]_{i+1,1}^T$ for time $i+1$ can be calculated from eqs (19) and (20) for $J = 1$.

Secondly, when J varies from 2 to N–1, the left- and right-running P and S waves across the Jth joint can be obtained from the waves caused by the two adjacent joints from eq. (21), that is, $[\, v_{rp}^- \; v_{rs}^- \,]_{i,J}^T = [\, v_{rp}^+ \; v_{rs}^+ \,]_{i-n_p,J-1}^T$ and $[\, v_{lp}^+ \; v_{ls}^+ \,]_{i+1,J}^T = [\, v_{lp}^- \; v_{ls}^- \,]_{i+1-n_p,J+1}^T$ For an incident S wave and $J = 2$, there is $[\, v_{rp}^{-}\ v_{rs}^{-}\,]_{i,2}^{T} = [\, v_{rp}^{+}\ v_{rs}^{+}\,]_{i-n_s,1}^{T}$. Combining the results in the previous steps, the right-running P and S waves, $[\, v_{rp}^{+}\ v_{rs}^{+}\,]_{i+1,J}^{T}$ ($J = 2{\sim}N{-}1$), at time $i + 1$ can be calculated from eqs (19) and (20) for the joints ranging from the second to the (N–1)th.

Thirdly, when J is N, there is no left-running P and S waves on the right-hand side of the joint, that is, $[\, v_{lp}^{+}\ v_{ls}^{+}\,]_{i,N}^{T} = [\,0\ 0\,]$. From eq. (21), the right-running P and S waves, v_{rp}^{-} and v_{rs}^{-}, on the left-hand side of the Nth joint can still be obtained from the waves emitted from the (N–1)th joint, that is, $[\, v_{rp}^{-}\ v_{rs}^{-}\,]_{i,N}^{T} = [\, v_{rp}^{+}\ v_{rs}^{+}\,]_{i-n_p,N-1}^{T}$. Hence, eqs (19) and (20) can give the reflected wave $[\, v_{lp}^{-}\ v_{ls}^{-}\,]_{i,1}^{T}$ at time i before the first joint and the transmitted waves $[\, v_{rp}^{+}\ v_{rs}^{+}\,]_{i+1,N}^{T}$ at time $i + 1$ after the Nth joint.

When the above three steps are repeated, the wave propagation across the N rock joints can be finally obtained in the whole time history. By applying this recursive method, the transmitted and the reflected waves across the joints in a rock mass can be calculated progressively by eqs (19)–(21).

To describe reflection and refraction, the transmission and reflection coefficients caused by an incident P or S wave are defined as,

$$T_{\eta-k} = \frac{\max\left|v_{lk,N}^{+}\right|}{\max\left|v_{l\eta,1}^{-}\right|}, \quad R_{\eta-k} = \frac{\max\left|v_{rk,1}^{-}\right|}{\max\left|v_{l\eta,1}^{-}\right|}, \tag{28}$$

where η denotes the incident P and S waves, that is, $\eta = p, s$; k denotes the P and S waves caused by the rock mass, that is, $k = p, s$; the subscripts r and l are for the right- and left-running waves, respectively.

3 SPECIAL CASES AND COMPARISONS

In this section, comparisons are conducted between the solutions from the proposed analytical method and the existing established analytical methods, by examining several cases. This also serves as a verification of the proposed method. Here, $K_n = k_n/(z_s\omega)$ and $K_s = k_s/(z_s\omega)$ are defined to be the normalized normal and tangential joint stiffness, respectively, where ω is the angle frequency of the incident waves.

3.1 Oblique incidence across a single joint

It is assumed that the rock mass contains only one single joint in this section. When the incident P or S waves obliquely impinges the rock joint, there is no left-running P and S waves on the right-hand side of the joint, that is, $v_{lp}^{+} = 0$ and $v_{ls}^{+} = 0$. Eqs (19) and (20) can be simplified as

$$\begin{bmatrix} v_{lp}^{-} \\ v_{ls}^{-} \end{bmatrix}_{i,1} = -B^{-1}A \begin{bmatrix} v_{rp}^{-} \\ v_{rs}^{-} \end{bmatrix}_{i,1} + B^{-1}A \begin{bmatrix} v_{rp}^{+} \\ v_{rs}^{+} \end{bmatrix}_{i,1} \tag{29}$$

$$\begin{bmatrix} v_{rp}^{+} \\ v_{ls}^{+} \end{bmatrix}_{i+1,1} = A^{-1}C \begin{bmatrix} v_{rp}^{+} \\ v_{rs}^{+} \end{bmatrix}_{i,1} + A^{-1}E \begin{bmatrix} v_{rp}^{-} \\ v_{rs}^{-} \end{bmatrix}_{i,1} + A^{-1}F \begin{bmatrix} v_{lp}^{-} \\ v_{ls}^{-} \end{bmatrix}_{i,1}, \tag{30}$$

where v_{rp}^{-} and v_{rs}^{-} denote the incident P and S waves, respectively. It is found that eqs (29) and (30) are in the same form with those by Li & Ma (2010), who derived the blast wave propagation equation for a linear rock joint. In order to verify the present method, the parameters adopted in the present study are the same as those by Gu *et al.* (1996), that is, $v = 0.2$, $K_n = K_s$ and $\beta_c = \sin^{-1}(c_s/c_p) = 37.8°$. The incidence is assumed to be sinusoidal P or S waves. Fig. 4 shows the variation of the transmission and reflection coefficients with the normalized joint stiffness, where Fig. 4(a) is for the incident P wave and Fig. 4(b) is for the incident S wave. In Fig. 4, the continuous curves are calculated by the proposed method and the scattered points are from the method by Gu *et al*. (1996), who studied the 2-D problem for one linear joint in frequency domain. By comparison, it is found that the results obtained by the two methods are exactly the same.

3.2 Normal incidence across a set of parallel joints

For incident P or S waves normally impinges a set of parallel joints, the transmitted waves can be calculated from eqs (19) to (21) when $\alpha \to 0$ and $\beta \to 0$. Assume there are four joints with joint spacing $S = \lambda_0/10$, where λ_0 is the wavelength and equal to c_p/f_0. The incident P wave is a half-cycle sinusoidal wave and the incident S wave is a one-cycle sinusoidal wave, that is,

$$I_p = \begin{cases} \sin(\omega t), & t = 0 \sim 1/(2f_0) \\ 0, & t > 1/(2f_0) \end{cases}, \quad \text{for incident } P \text{ waves} \tag{31}$$

$$I_s = \begin{cases} \sin(\omega t), & t = 0 \sim 1/f_0 \\ 0, & t > 1/f_0 \end{cases}, \quad \text{for incident } S \text{ waves,} \tag{32}$$

where $\omega = 2\pi f_0$ and $f_0 = 100$ Hz.

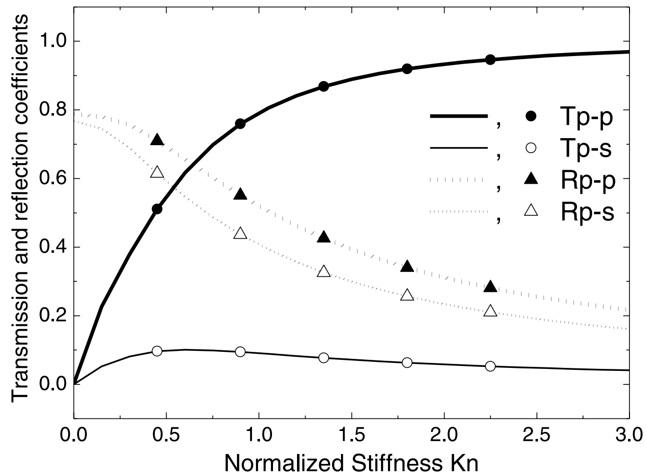

(a) Incident P-wave

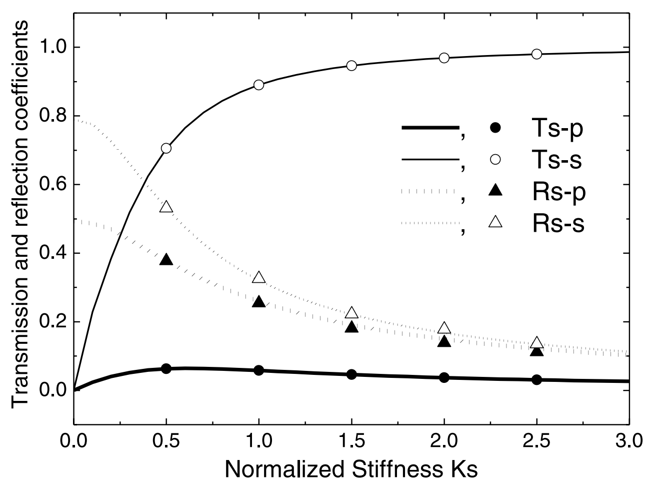

(b) Incident S-wave

Figure 4. Comparison of the transmitted waves for an oblique incidence across a single rock joint. The continuous curves are from the proposed recursive method and the scattered points are from the method by Gu *et al.* (1996).

The calculation results are compared with those obtained by the methods of Zhao *et al*. (2006a,b) and Li *et al.* (2010, 2011). On the basis of the displacement discontinuity model and the characteristic line theory, Zhao *et al.* (2006a,b) derived the wave propagation equation for an incident *P* or *S* wave across a set of parallel joints with linearly elastic or Coulomb-slip behaviour. The wave propagation equations obtained by Zhao *et al.* (2006a,b) were in time domain. Li *et al.* (2010, 2011) proposed an equivalent viscoelastic medium model for a rock mass with a set of parallel joints, which are linearly elastic. This equivalent model includes a viscoelastic model and the concept of the virtual wave source, and can directly be adopted to analyse *P*- or *S*-wave propagating normally across parallel joints in frequency domain. Figs 5(a) and (b) show the computation results by the present method and the comparisons for incident *P* and *S* waves. It can be seen from Fig. 5 that the present results are consistent with those by the methods of Zhao *et al.* (2006a,b) and Li *et al.* (2010, 2011). Therefore, the wave propagation equations derived in the present study are proven to be effective to study plane *P*- or *S*-wave propagation across a rock mass with a set of parallel joints.

4 APPLICABILITY AND ADVANTAGE

The time-domain recursive method has the advantage over the other existing analytical methods, reflected primarily by its wider applicability on parametric studies and computational efficiency. The former is of particular importance as in many cases, such as the effects of various wave or loading parameters on wave propagation in a jointed medium.

The examples given in this section is to illustrate, through the analyses on incident waveform, impinging angle and loading duration, the applications of this recursive methods in studying wave propagation with more complex configurations. In the examples, the normal

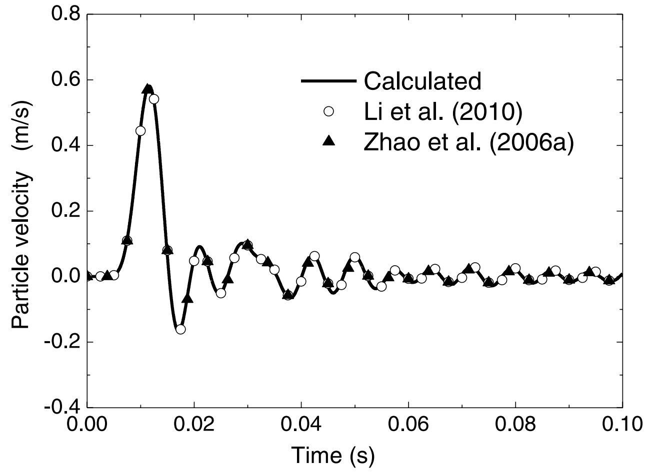

(a) Incident P-wave

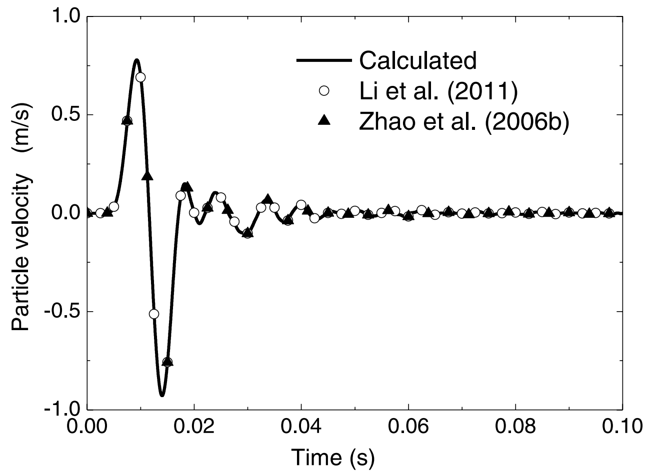

(b) Incident S-wave

Figure 5. Comparison of the transmitted waves for a normal incidence across rock joints.

and tangential stiffness are still assumed to be identical and $k_s = k_n$ =3.5 GPa m^{-1}, rock density ρ is 2650 kg m^{-3}, *P*-wave velocity α_p is 5746.2 m s^{-1} and shear wave velocity α_s is 3071.5 m s^{-1}, the joint spacing *S* is $\lambda_0/10$. The applicability of the recursive method presented in Section 2.3 will also be studied for soft and stiff joints.

4.1 Effect of incident waveform

For an incidence with an arbitrary waveform, the Fourier and the inverse Fourier transforms were usually needed to calculate the transmitted waves (Achenbach 1973), while the recursive method can directly give the transmitted wave for an incidence with an arbitrary waveform without additional mathematical methods. The incidences shown in Fig. 1 are assumed to be half-cycle sinusoidal, triangular and rectangular pulses with the peak value in one unit and the same loading duration. The impinging angles are $\alpha = 20^\circ$ and $\beta = 10.5^\circ$ for the incident *P* and *S* waves, respectively. The incidence is the right-running *P* or *S* wave in eqs (19) and (20). When there are four or 20 rock joints, that is, $N = 4$ or 20, the recursive method presented in Section 2.3 can directly be used to solve the transmitted *P* and *S* waves, as shown in Figs 6–8 for the incident *P* or *S* waves with three waveforms, respectively. Difference is observed among the transmitted *P* or *S* waves for the three incident *P* or *S* waves.

4.2 Effect of impinging angle and loading duration

In the following exercise, the incident *P* and *S* waves with functions defined by eqs (31) and (32) will be adopted, and the joint number *N* is assumed to be four. The loading duration t_d of the incident *S* wave is $1/f_0$, which is twice that of the incident *P* wave.

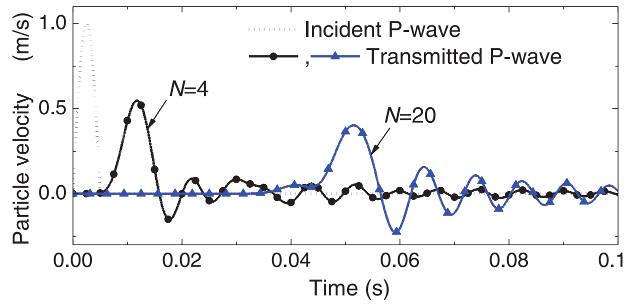

(a) Transmitted P-waves for an incident P-wave

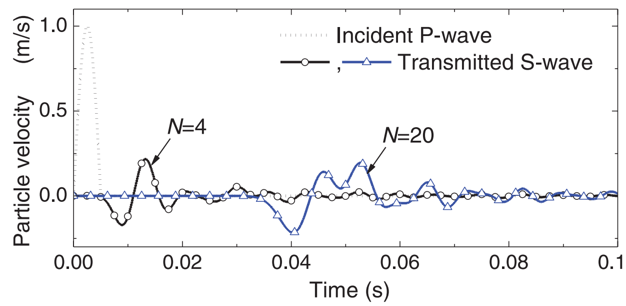

(b) Transmitted S-waves for an incident P-wave

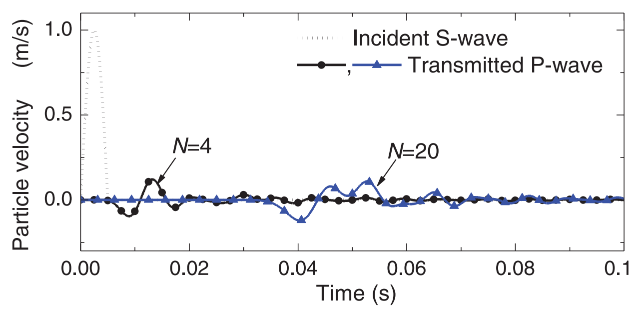

(c) Transmitted P-waves for an incident S-wave

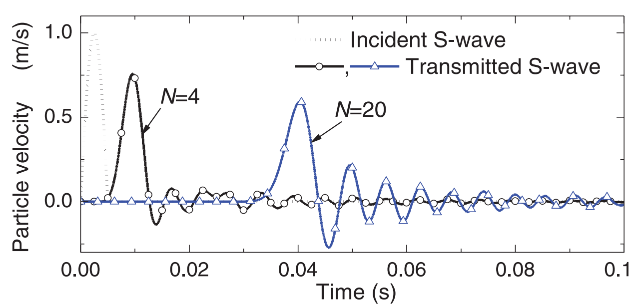

(d) Transmitted S-waves for an incident S-wave

Figure 6. Transmitted waves for a half-cycle sinusoidal incident *P* or *S* wave.

When v_{rp}^- and v_{rs}^- on the first joint are respectively evaluated as the incident *P* and *S* waves, the transmitted and reflected waves can be calculated from the recursive equations (19) to (21), and hence the corresponding transmission and reflection coefficients for a given impinging angle are obtained from eq. (28). Fig. 9 shows the variation of transmission and reflection coefficients with the impinging angle. Fig. 9 shows that the transmission and reflection coefficients change with varying incident angle until the incident angles are close to the critical angles, that is, $\alpha_c = 90^\circ$ and $\beta_c = 32.3^\circ$.

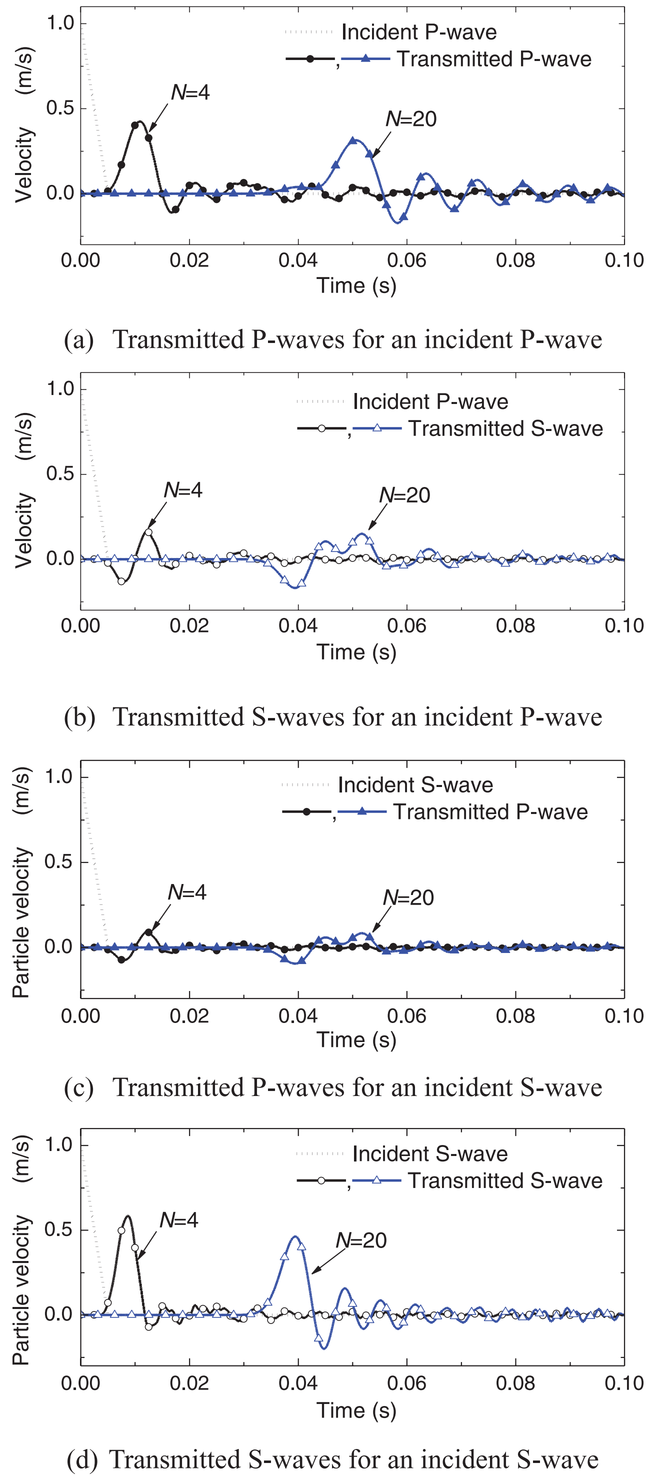

Figure 7. Transmitted waves for a triangular incident *P* or *S* wave.

When the impinging angles are $\alpha = 20^\circ$ and $\beta = 10.5^\circ$, the recursive equations (19) to (21) and eq. (28) can also be applied to calculate the transmission and reflection coefficients for a loading duration t_d. The variations of the transmission and reflection coefficients with t_d are shown in Figs 10(a) and (b) for the incident *P* and *S* waves, respectively.

4.3 Limit cases of joint stiffness

The recursive method can be used to analyse the limit joint stiffness. For joints with low stiffness, that is, $k_n \rightarrow 0$ and $k_s \rightarrow 0$, from eq. (20), the left- and right-running *P* and *S* waves on the right-hand side of the joints must be zero to keep the equality of equation, which means that there are no *P* and *S* waves emitted from the right-hand side of the joints. According to the time-shifting function eq. (21), there are also no *P*

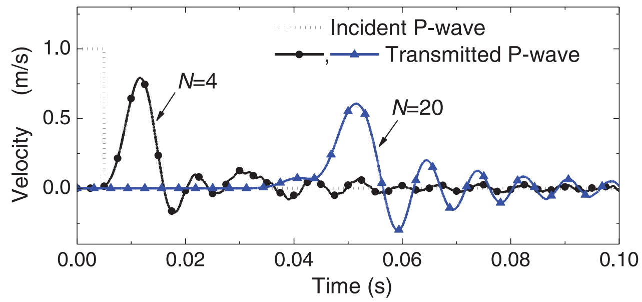

(a) Transmitted P-waves for an incident P-wave

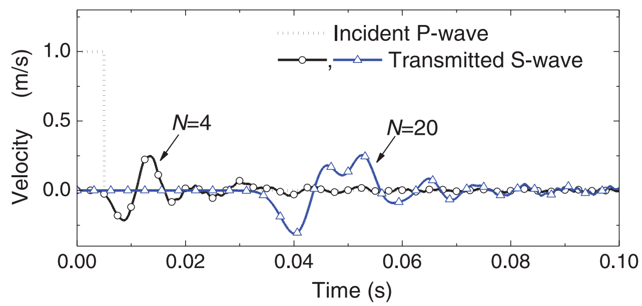

(b) Transmitted S-waves for an incident P-wave

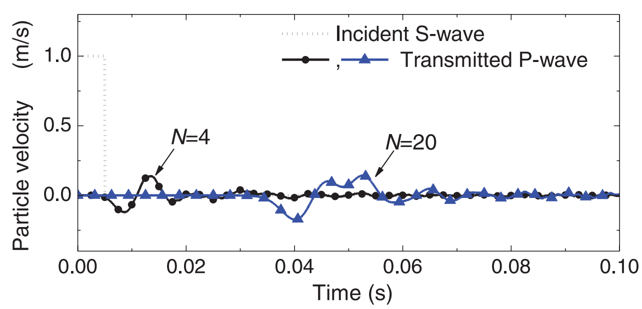

(c) Transmitted P-waves for an incident S-wave

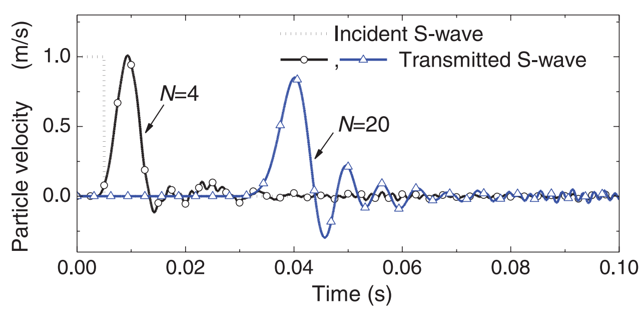

(d) Transmitted S-waves for an incident S-wave

Figure 8. Transmitted waves for a rectangular incident *P* or *S* wave.

and *S* waves given rise from the left-hand side of the joints except for the first joint. If the incident waves in Fig. 1 are known, the left-running *P* and *S* waves on the left-hand side of the first joint can be calculated from eq. (19). In another word, the incidence in Fig. 1 is completely reflected to be the left-running *P* and *S* waves when the joint stiffness is very small. For this case, the joints act as a free surface, from which only reflected *P* and *S* waves are emitted from the first joint interface.

For very stiff joints, that is, when $k_n \rightarrow \infty$ and $k_s \rightarrow \infty$, from eq. (20), there are $v_{rp}^{+} = v_{rp}^{-}$, $v_{rs}^{+} = v_{rs}^{-}$, $v_{lp}^{+} = v_{lp}^{-}$ and $v_{ls}^{+} = v_{ls}^{-}$, which means all the incident waves propagate across the rock joints without any changes. For this case, the interface of a joint is considered to be welded and the rock mass is continuous.

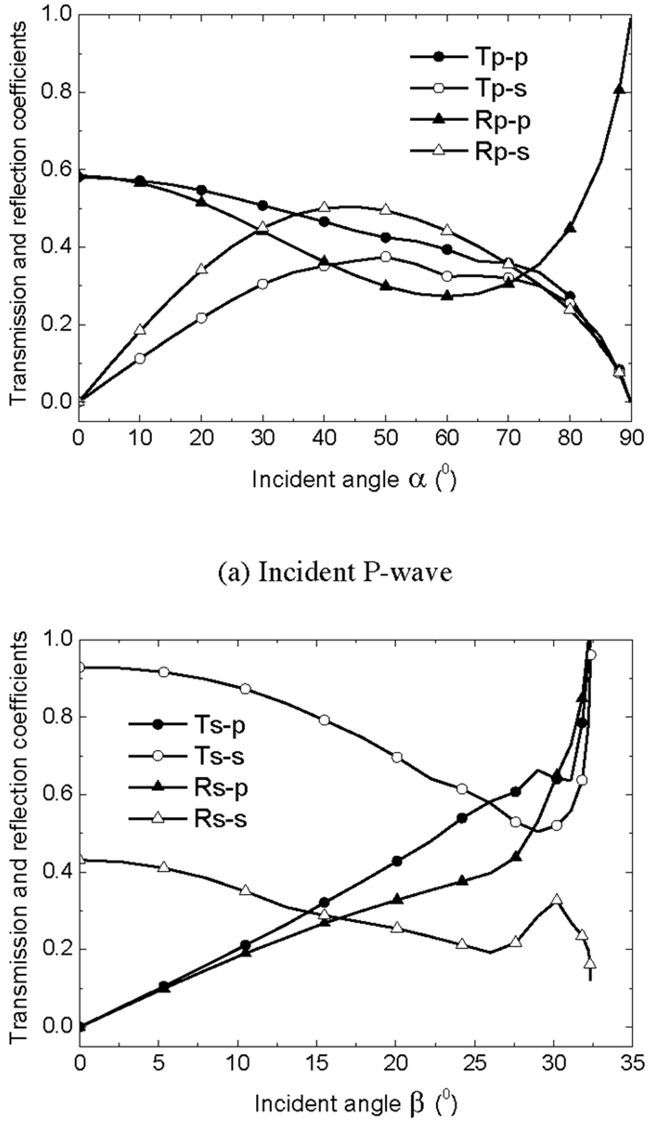

(b) Incident S-wave

Figure 9. Effect of the incident angle on transmission and reflection coefficients.

4.4 Other applications and limitations

The proposed recursive method is used in the above given examples to analyse transient waves propagating across linearly deformable rock joints. Moreover, the method can be applied to other waves (e.g. earthquake waves) and to more complex joints (e.g. nonlinearly deformable and viscoelastic behaviour).

It should be noted that the proposed recursive method can only be applicable to the incidence with impinging angles less than the critical angles, that is, $0 \leq \alpha < \alpha_c$ and $0 \leq \beta < \beta_c$. When $\alpha = \alpha_c$ or $\beta \geq \beta_c$, the interface waves will be generated and propagate on the interface of the joints. The recursive method does not include interface wave analysis.

5 CONCLUSIONS

To efficiently investigate the effect of multiple joints on transient *P*- and *S*-wave propagation across a rock mass, a time-domain recursive method is adopted to express the wave propagation equation when the impinging angles are less than the critical impinging angles. In the present study, the interaction between the *P* and *S* waves with a joint is first analysed according to the displacement field for plane wave propagation across a set of parallel rock joints. By comparison with some special cases, such as oblique incidence across a single joint and normal incidence across multiple joints, the proposed method and the derived wave propagation equation are proved to be effective to study wave propagation in jointed rock masses. The proposed method can be directly applied for any incident wave with different waveform without

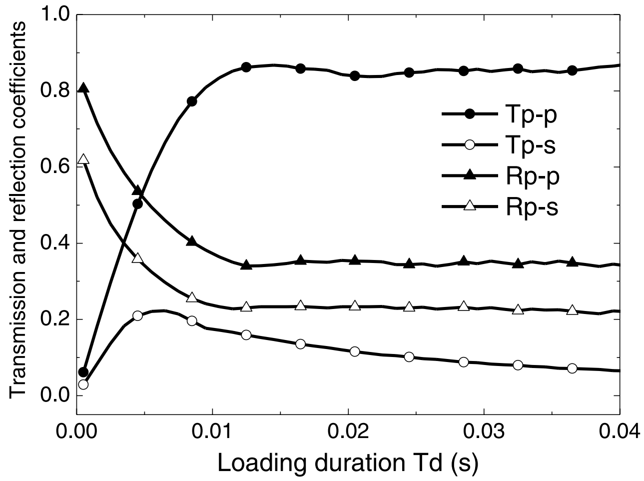

(a) Incident P-wave

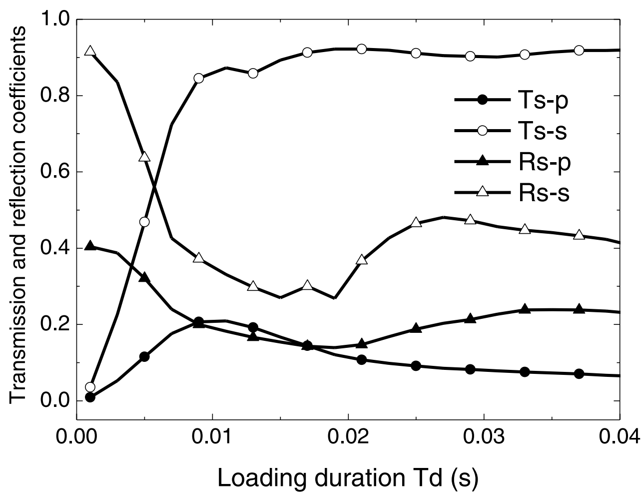

(b) Incident S-wave

Figure 10. Effect of the loading duration on transmission and reflection coefficients.

losing precision. Meanwhile, the method can be used to calculate the transmission and reflection coefficients for incidences with different impinging angle and loading duration. By discussions on the effects of the soft and rigid joints on wave propagation, we also find that the analytical method proposed in the paper is reasonable and effective. Since the other mathematical methods, such as the Fourier and the inverse Fourier transforms, are not involved, the calculating efficiency prominently increases.

ACKNOWLEDGMENTS

The study is supported by Chinese National Science Research Fund (11072257, 51025935) and the Major State Basic Research Project of China (2010CB732001). The authors also thank Dr Jianbo Zhu of EPFL Switzerland for the useful discussions.

REFERENCES

Achenbach, J.D., 1973. *Wave Propagation in Elastic Solids,* Elsevier, New York, NY.

Aki, K. & Richards, P.G., 2002. *Quantitative Seismology,* University Science Books, Mill Valley, CA.

Bedford, A. & Drumheller, D.S., 1994. *Introduction to Elastic Wave Propagation,* Wiley & Sons, Chichester.

Ewing, W.M., Jardetzky, W.S. & Press, F., 1957. *Elastic Wave in Layered Media,* McGraw-Hill, New York, NY.

Fuchs, K. & Müller, G., 1971. Computation of synthetic seismograms with reflectivity method and comparison with observation, *Geophys. J. Int.,* **23**(4), 417–433.

Gu, B.L., SuarezRivera, R., Nihei, K.T. & Myer, L.R., 1996. Incidence of plane waves upon a fracture, *J. geophys. Res.,* **101**(B11), 25 337–25 346.

Kennett, B.L.N. & Kerry, N.J., 1979. Seismic waves in a stratified half space, *Geophys. J. Int.,* **57**(3), 557–583.

Kolsky, H., 1953. *Stress Waves in Solids,* Clarendon Press, Oxford.

Li, J.C. & Ma, G.W., 2010. Analysis of blast wave interaction with a rock joint, *Rock Mech. Rock Eng.,* **43**(6), 777–787.

Li, J.C., Ma, G.W. & Zhao, J., 2010. An equivalent viscoelastic model for rock mass with parallel joints, *J. geophys. Res.,* **115,** B03305, doi:10.1029/2008JB006241.

Li, J.C., Ma, G.W. & Zhao, J., 2011. Equivalent medium model with virtual wave source method for wave propagation analysis in jointed rock masses, in *Advances in Rock Dynamics and Applications,* Chapter 10, eds Zhou, Y.X. & Zhao, J., Taylor & Francis Group, London.

Luco, J.E. & Apsel, R.J., 1983. On the green-functions for a layered half-space. Part I, *Bull. seism. Soc. Am.,* **73**(4), 909–929.

Miller, R.K., 1977. An approximate method of analysis of the transmission of elastic waves through a frictional boundary, *J. appl. Math.,* **44**(4), 652–656

Perino, A., Zhu, J.B., Li, J.C., Barla, G. & Zhao, J., 2010. Theoretical methods for wave propagation across jointed rock masses, *Rock Mech. Rock Eng.,* **43**(6), 799–809.

Pyrak-Nolte, L.J., Myer, L.R. & Cook, N.G.W., 1990a. Transmission of seismic-waves across single natural fractures, *J. geophys. Res.,* **95**(B6), 8617–8638.

Pyrak-Nolte, L.J., Myer, L.R. & Cook, N.G.W., 1990b. Anisotropy in seismic velocities and amplitudes from multiple parallel fractures, *J. geophys. Res.,* **95**(B7), 11 345–11 358.

Schoenberg, M., 1980. Elastic wave behavior across linear slip interfaces, *J. acoust. Soc. Am.,* **68**(5), 1516–1521.

Zhao, J. & Cai, J.G., 2001. Transmission of elastic P-waves across single fractures with a nonlinear normal deformational behavior, *Rock Mech. Rock Eng.,* **34**(1), 3–22.

Zhao, X.B., Zhao, J. & Cai, J.G., 2006a. P-wave transmission across fractures with nonlinear deformational behaviour, *Int. J. Numer. Anal. Methods Geomech.,* **30**(11), 1097–1112.

Zhao, X.B., Zhao, J., Hefny, A.M. & Cai, J.G., 2006b. Normal transmission of S-wave across parallel fractures with Coulomb slip behavior, *J. Eng. Mech.-ASCE,* **132**(6), 641–650.

Zhu, J.B., Perino, A., Zhao, G.F., Barla, G., Li, J.C., Ma, G.W. & Zhao, J., 2011. Seismic response of a single and a set of filled joints of viscoelastic deformational behaviour, *Geophys. J. Int.,* **186,** 1315–1330.